



Mechanical properties, drying and autogenous shrinkage of blast furnace slag activated with hydrated lime and gypsum

Antonio A. Melo Neto^{a,*}, Maria Alba Cincotto^b, Wellington Repette^c

^a Department of Civil Engineering, Federal University of Pernambuco (UFPE), BR 104 KM 59, 55002-970 Caruaru, Pernambuco, Brazil

^b Department of Civil Construction Engineering, University of São Paulo (USP), Av. Prof. Almeida Prado 83, 05508-900 São Paulo, São Paulo, Brazil

^c Department of Civil Engineering, Federal University of Santa Catarina (UFSC), 88040-900 Florianópolis, Santa Catarina, Brazil

ARTICLE INFO

Article history:

Received 24 April 2008

Received in revised form 18 January 2010

Accepted 22 January 2010

Available online 1 February 2010

Keywords:

Blast furnace slag

Activation

Autogenous shrinkage

Drying shrinkage

Porosimetry

Thermal Analysis

ABSTRACT

This article reports the characteristics of blast furnace slag (BFS) pastes activated with hydrated lime (5%) and hydrated lime (2%) plus gypsum (6%) in relation to compressive strength, shrinkage (autogenous and drying) and microstructure (porosity, hydrated products). The paste mixtures were characterized using powder X-ray diffraction (XRD), mercury intrusion porosimetry (MIP) and thermogravimetric analysis (TG/DTG). BSF activated with lime and gypsum (LG) results in larger amounts of ettringite when compared with BFS activated with lime (L). Although the porosities of the L and LG mixtures were about the same, there was a greater pore refinement for the BFS activated with lime, with an increase in mesopores volume with age. The presence of ettringite and the higher volumes of macropores cause the compressive strength of BSF activated with hydrated lime plus gypsum to be smaller than that of BFS activated with lime. For both chemical activators, compressive strength developed slowly at early ages. Autogenous and drying shrinkage were greater for the BFS activated with lime, believed to result from the more refined porous structure in comparison with the mixture activated with gypsum plus lime.

© 2010 Elsevier Ltd. All rights reserved.

1. Introduction

The development of new materials and technologies that incorporate residues has become an important industry goal and among the various residues under study, blast furnace slag (BFS) plays a very important role. Moreover, even though the Brazilian cement industry consumes a significant amount of BFS, there is still a great volume available for use as an alternative binder. According to the Brazilian Steel Institute, the annual production of pig iron in Brazil increased significantly, 35% in the last 5 years, reaching around 34 million tons in 2008. According to this data, it is estimated that the amount of blast furnace slag generated in the production of pig iron is around 10 million tons per year. Since, approximately, 70% of this amount is being used by the cement manufactories to produce different types of Portland cement, only in Brazil around three million tons per year of slag are still available for other applications, including the production of slag cements. As it is known, BFS needs to be chemically or mechanically activated in order to hydrate into a hardened and durable material [1–6]. Currently, the activation of slag by sodium silicate is that most frequently studied because

the obtained BFS cement achieves higher and faster compressive strengths, compared with that of ordinary Portland cements (OPC) [7–10]. However, there are some applications where early strength development is not always required. For instance, in the production of vegetal fiber composites, one of the main aspects is the degradation of the fibers due to the matrix [11–13], resulting in a lower mechanical performance of the material. Blast furnace slag activated with hydrated lime or gypsum with lime [14,15], produces a lower alkalinity of the pore water compared to that of OPC or BFS activated by sodium silicate [16,17]. The advantage of this alternative binder over Portland cement was evidenced by a study of panels produced using mortar reinforced with coconut fiber; the binder was BFS activated by 2% lime and 10% gypsum [18]. After 12 years, the fibers remained undamaged, as it was observed by scanning electron microscopy (SEM) analysis. Other application would be in the concreting of massive structures, e.g. concrete dams, as the heat of hydration for the gypsum and for the lime activated gypsum systems tend to be smaller than that of the OPC or BFS activated by sodium silicate. The object of the present work was to determine the effects of hydrated lime and hydrated lime plus gypsum on the activation of BFS cements, particularly in relation to their mechanical properties, heat of hydration, microstructure and drying and autogenous shrinkage.

* Corresponding author. Tel.: +55 81 4105 0625; fax: +55 11 3091 5544.

E-mail address: antonio.meloneto@ufpe.br (A.A.M. Neto).

2. Experimental

2.1. Materials and mix proportion of mortars and pastes

The granulated blast furnace slag was supplied by Companhia Siderúrgica de Tubarão, with a basicity coefficient of $K_b = (CaO + MgO)/(SiO_2 + Al_2O_3) = 1.21$. The slag consisted of 99.5% glass with an amorphous halo angle of around $2\theta = 30^\circ$ and crystalline compounds, namely gehlenite and merwinite (Fig. 1). The BFS chemical composition and physical characteristics are shown in Table 1. The aggregate used was quartz sand (density = 2.62 g/cm^3) composed of four equal proportions of the fractions sieved (Table 2).

Mortar samples were prepared with a mass proportion of cementitious binder:sand:water of 1:2:0.48, while the paste samples were prepared with a mass proportion of 1:0.48. The cementitious binder corresponds to the total mass of slag and activators: (a) activator L – hydrated lime (5%, by slag mass); (b) mixed activator LG – hydrated lime (2%, by slag mass) plus gypsum (6%, by slag mass). Tables 3 and 4 show, respectively, the chemical compositions of hydrated lime and natural gypsum as determined by chemical and thermogravimetric analysis.

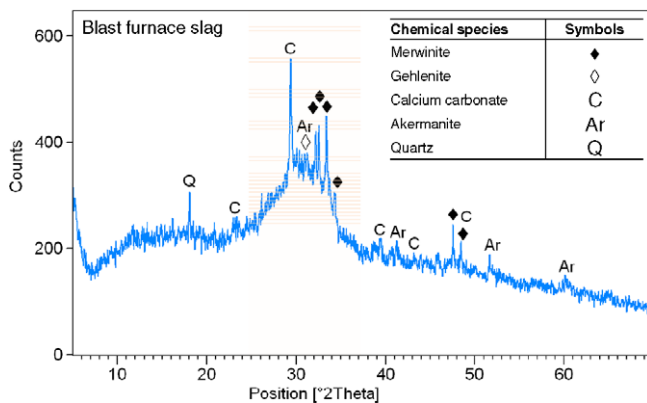


Fig. 1. X-ray diffractogram of the blast furnace slag.

Table 1

Blast furnace slag physical characteristics and chemical composition.

Physical characteristics

Density: 2.88 g/cm³

Blaine finesses: 500 m²/kg

Specific surface area (laser granulometry): 493 m²/kg

Average particle diameters

$D_{10} = 2.22$, $D_{50} = 11.88$, $D_{90} = 32.46$, $D_{[4.3]} = 15.02$, $D_{[3.2]} = 4.59$

Chemical composition (%)

CaO	44.20	TiO ₂	0.59
SiO ₂	32.50	Fe ₂ O ₃	0.53
Al ₂ O ₃	10.10	MnO	0.45
MgO	7.45	K ₂ O	0.37
SO ₃	2.41	LOI	0.95

Table 2

Percentage by weight corresponding to sand granulometry fractions (mm).

>4.8 mm	4.8–2.4 mm	2.4–1.2 mm	1.2–0.6 mm	0.6–0.3 mm	0.3–0.15 mm	<0.15 mm
0	0	25	25	25	25	0

2.2. Testing methods

Changes in hydrated compounds and microstructure due to the evolution of hydration were determined in paste samples prepared with a water/binder ratio of 0.48. The arrest of hydration took place by freezing the samples in liquid nitrogen, followed by lyophilization for the removal of water. For each mixture, samples were prepared at the hydration ages of 1, 3, 7, and 28 days. Thermogravimetric curves were obtained using a NETSZCH TG 209-C thermobalance, at a heating rate of $10^\circ\text{C}/\text{min}$ under a nitrogen atmosphere with a gas flux of $30 \text{ ml}/\text{min}$. For this test, samples were first ground, and only the particles retained by the sieves sized between $75 \mu\text{m}$ and $150 \mu\text{m}$ mesh, were used.

Pore size distribution was determined by using a Micromeritics Autopore III 9410 porosimeter under pressures ranging from zero to 414 MPa . The assumed surface tension of the mercury was 0.485 N/m at 25°C (ASTM D 4404-84). The density of the mercury was 13.5413 g/ml and the assumed contact angle 130° . For the calorimetry tests, samples of paste were prepared by mixing 20 g of slag and water + activator in a plastic bag before being immediately transferred to a JAF Wexham conduction calorimeter at 20°C . As the mixture was prepared outside the equipment, the wetting peak could not be determined.

Nine mortar prisms of $25 \times 25 \times 285 \text{ mm}$ were cast for each binder and for each type of shrinkage test, drying and autogenous. Length and mass evolutions were determined according to ASTM C490, at the ages of 1, 2, 3, 4, 5, 6, 7, 9, 11, 14, 21 and 28 days. To avoid moisture evaporation during the autogenous shrinkage test, all prisms were wrapped in two layers: the first one, a plastic sheet, and then an outer layer an aluminum foil, sealed with aluminum tape. The maximum moisture loss recorded was 0.2% after 56 days. The prisms were demolded over a 24 h period for autogenous and drying shrinkage and immediately stored in a dry room at a constant temperature of 24°C and $50\% \text{ RH}$. The maximum rise in temperature of the specimens (measured by inserting type K thermocouples into dummy specimens) due to heat released during hydration was 3°C . All drying and autogenous shrinkage results were corrected to account for the effects of temperature considering a thermal expansion coefficient equal to $15 \times 10^{-6}/^\circ\text{C}$ [9]. The compressive strength was measured according to BS EN-

Table 3
Hydrated lime chemical composition.

Compound	Weight percent
Ca(OH) ₂	91
Mg(OH) ₂	0.56
CaSO ₄	0.49
CaCO ₃	5.60
SiO ₂	1.50
Al ₂ O ₃ + Fe ₂ O ₃	0.89
Free water	0.36
(CaO + MgO)	92

Table 4
Natural gypsum chemical composition.

Compound	Weight percent
CaSO ₄ ·2H ₂ O	88.90
CaSO ₄	7.12
CaCO ₃	1.54
MgCO ₃	0.42
MgO	0.16
SiO ₂ + Al ₂ O ₃ + Fe ₂ O ₃	0.84

196, at the ages of 1, 3, 7, 14, 21, 28 and 56 days. Six mortar cubes of $4 \times 4 \times 4$ (cm) were cast for each binder and demolded after 24 h of curing and then stored in a room at a constant temperature of 24 °C and 100% RH until testing age.

3. Results and analyses

3.1. Hydration evolution heat

Fig. 2a shows the profile of cumulative heat evolution during the first 72 h. The LG mix has a greater cumulative heat than that of L mix which occurs due to the formation of ettringite and its subsequent transformation in monosulfoaluminate; the presence of both confirmed by X-ray diffraction (XRD) [16–18]. Fig. 2b presents kinetic reaction curves. The first peak is an indication of the early dissolution of the slag and almost an absence of induction period. The second one occurs around 12 h for both mixes, but it is higher for the LG mix due to the formation of ettringite. The third peak, occurring at around 30 h, and only for the LG mix, is attributed to the transformation of ettringite into monosulfoaluminate [19]. The total heat released at 72 h observed in the slag activated

by lime (80 kJ/kg) or with lime plus gypsum (90 kJ/kg) is much smaller than that observed in an ordinary cement Portland, around 300 kJ/kg [9,20]. This fact confirms the possibility of using this type of cement in massive gravity concrete dams.

3.2. Thermogravimetry analyses

In both mixtures, the results of thermogravimetry analysis (TGA) (Figs. 3a and 4a) show that mass loss increases with the age of hydration reactions. In the L mixture (Fig. 3b), the results indicate a mass loss peak between 30 °C and 220 °C that is attributed to C–S–H (I) and aluminate phases. There is also a mass loss peak related to the decomposition of uncombined calcium hydroxide between 375 °C and 500 °C, and the occurrence of a mass loss peak due to the decomposition of uncalcined calcium carbonate from hydrated lime, at temperatures near 700 °C.

The LG mixture presents an expressive loss of mass between 30 °C and 220 °C (Fig. 4b) related to the decomposition of ettringite, at around 100 °C [19], and C–S–H. A smooth mass loss peak related to the decomposition of the aluminate phases (hydratocalyte, AFm) appears between 275 °C and 420 °C, and the occurrence of a mass loss peak due to the decomposition of calcium carbonate was observed at temperatures around 700 °C. The main difference between the L and LG mixes was a profuse formation of ettringite [16–18,21] in the LG mixture, which affected its mechanical properties. Another difference is related to the calcium hydroxide peak that is not observed in the slag activated by lime plus gypsum. The absence of calcium hydroxide peak in the LG mixture is attributed to its consumption by the hydration reactions and also by its smaller utilized amount (2%) compared to that used for L mixture (5%).

3.3. Porosity

In Fig. 5a, the cumulative curves of pore size distribution show a refinement of the pores in relation to hydration time for the L mixture. This mixture presents a higher volume of pores in the mesopores interval (Fig. 5b–d) that directly affects its mechanical properties, mainly compressive strength and shrinkage. The amount of large mesopores (Fig. 5b–d) remains almost constant over the time, however there is a more intense refinement of the pore structure in 28 days, resulting in an increase of the amount of small mesopores. The porosity characteristics of this mixture are attributed to the hydration development over the time and to the main hydrated products formed, C–S–H, and added calcium

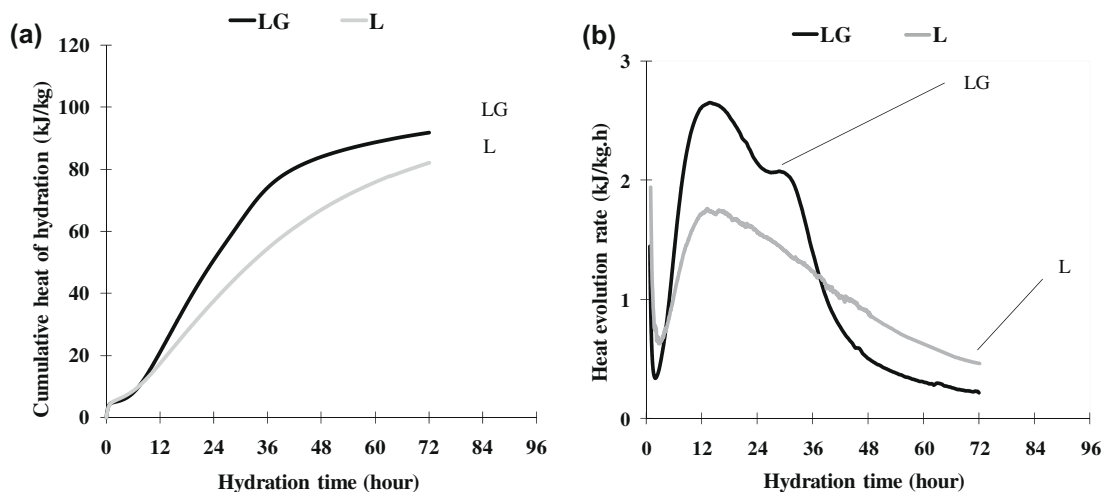


Fig. 2. Cumulative heat of hydration (a) and heat evolution rate (b) of slag cement.

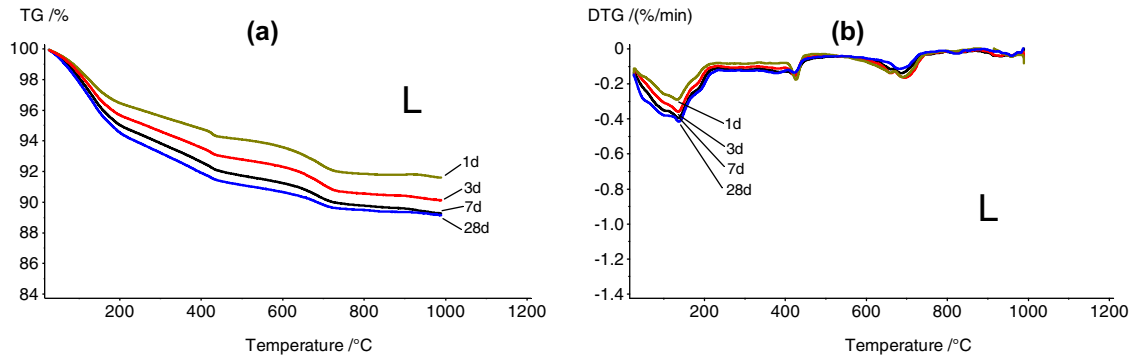


Fig. 3. TG (a) and DTG (b) curves of L mixture in 1, 3, 7 and 28 days.

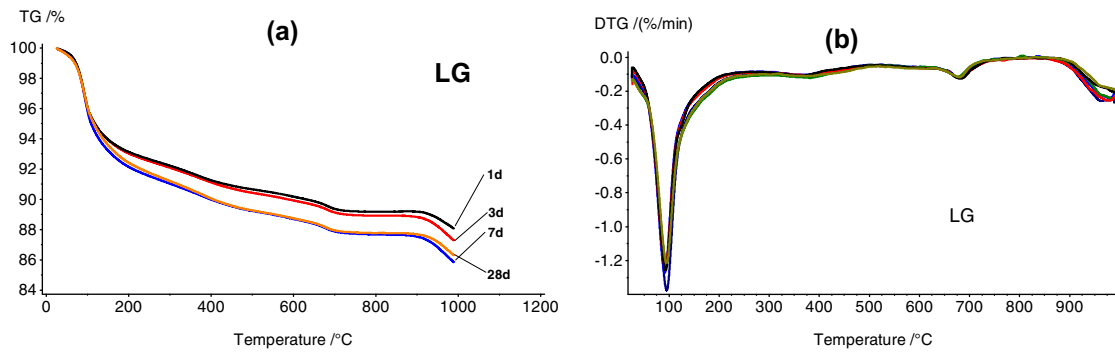


Fig. 4. TG (a) and DTG (b) curves of LG mixture in 1, 3, 7 and 28 days.

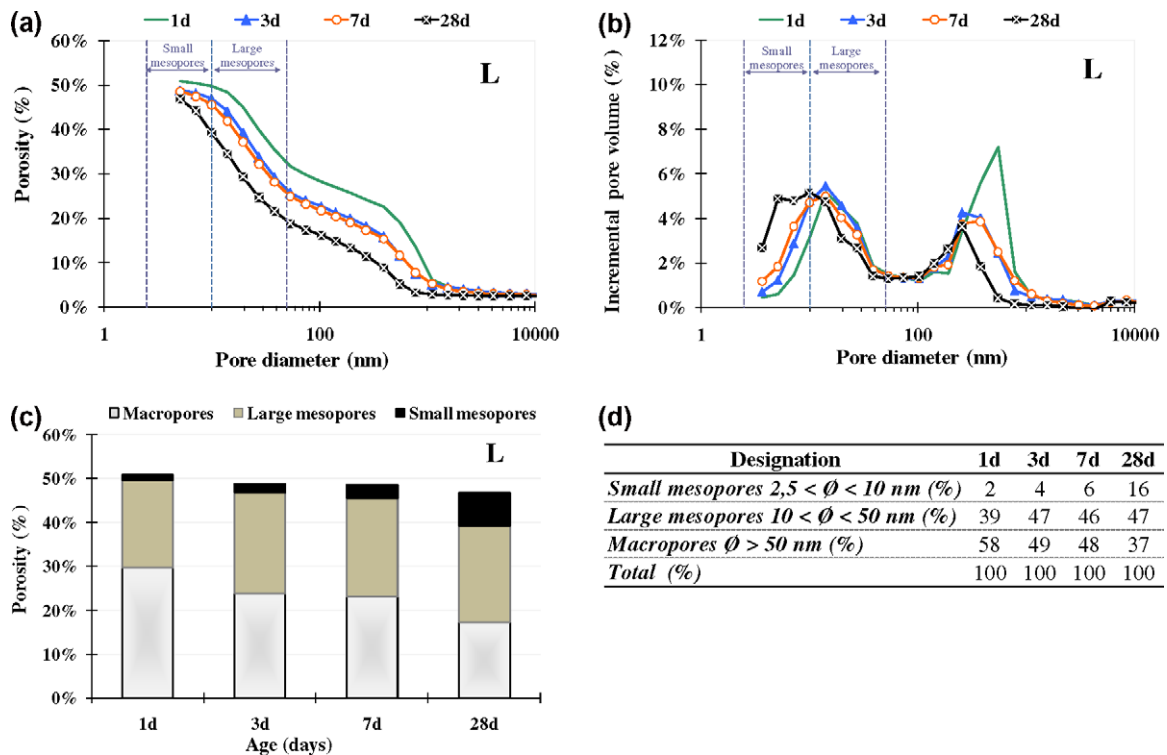


Fig. 5. Porosity (a), incremental pore size (b), porosity distribution (c) and percentile frequency of L mixture in 1, 3, 7 and 28 days.

hydroxide. Because ettringite is not formed when slag is activated by lime, it is reasonable to suppose that the presence of ettringite is related to pore structure behavior of the slag activated by lime plus gypsum when compared with the slag activated by lime only.

Regarding the incremental pore volume, it is observed that the L mixture showed a bimodal profile at all ages studied, with a peak between the diameters of 100 nm and 10,000 nm and a peak located between the diameters of 1 nm and 100 nm (Fig. 5b). The LG mixture presents a unimodal curve profile with a peak located between the diameters of 100 nm and 10,000 nm (Fig. 6b). The LG mixture reveals a higher porosity (Fig. 6a) and a greater frequency of pores out of the mesopores interval than the L mixture (Fig. 6b–d). Therefore, according to the results it is evident that the LG mixture porosity is less refined than the L mixture with water. This difference is due to the nature of the hydrated products in LG, formed with a greater content of ettringite, causing an increase in porosity and a more open matrix [22], different from the L mixture. The pore size distribution associated with hydrated product nature explains the compressive strength and shrinkage differences between the slag activated by lime and activated by lime plus gypsum.

3.4. Compressive strength

The compressive strength of the L mixture was greater than that of LG (Fig. 7); however, the LG mixture presents greater mass loss in the range regarding C–S–H and ettringite content, as shown by thermogravimetric results. The nature of the hydrated products explains this: the main hydrated products for the L mixture are C–S–H and portlandite, while for LG they are C–S–H and ettringite, of which there is a significant amount. Therefore, in the LG mixture, the mass loss between 30 °C and 220 °C is mostly attributed to the dehydration of ettringite. Another important contribution to the greater compressive strength of the L mixture is the pore size frequency situated in the mesopores range. With the same total

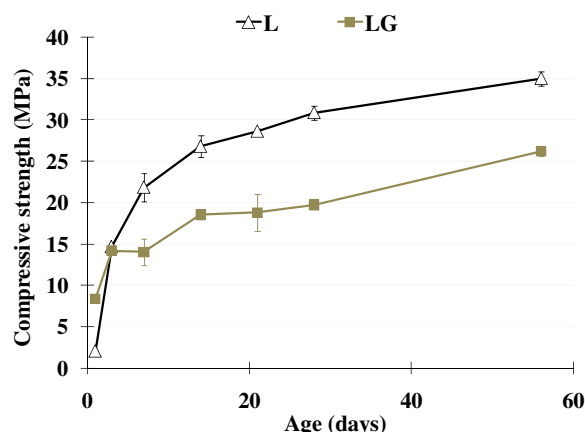


Fig. 7. Compressive strength of L mixture and LG mortars.

pore volume, the L mixture has around 57% more mesopores than the LG mixture.

3.5. Drying and autogenous shrinkage

The plotted curves in Figs. 8 and 9 correspond to the average drying and autogenous shrinkage results of nine replicate specimens for each mix. The cumulative drying and autogenous shrinkage for the L mixture is greater than in the LG mixture. In both mixtures, most of the total drying and autogenous shrinkage takes place. When comparing activation using hydrated lime plus gypsum (LG mixture) with activation using hydrated lime (L mixture) results in a decrease of total porosity and an increase in mesopores volume which is directly related to the increase of shrinkage due to self-desiccation.

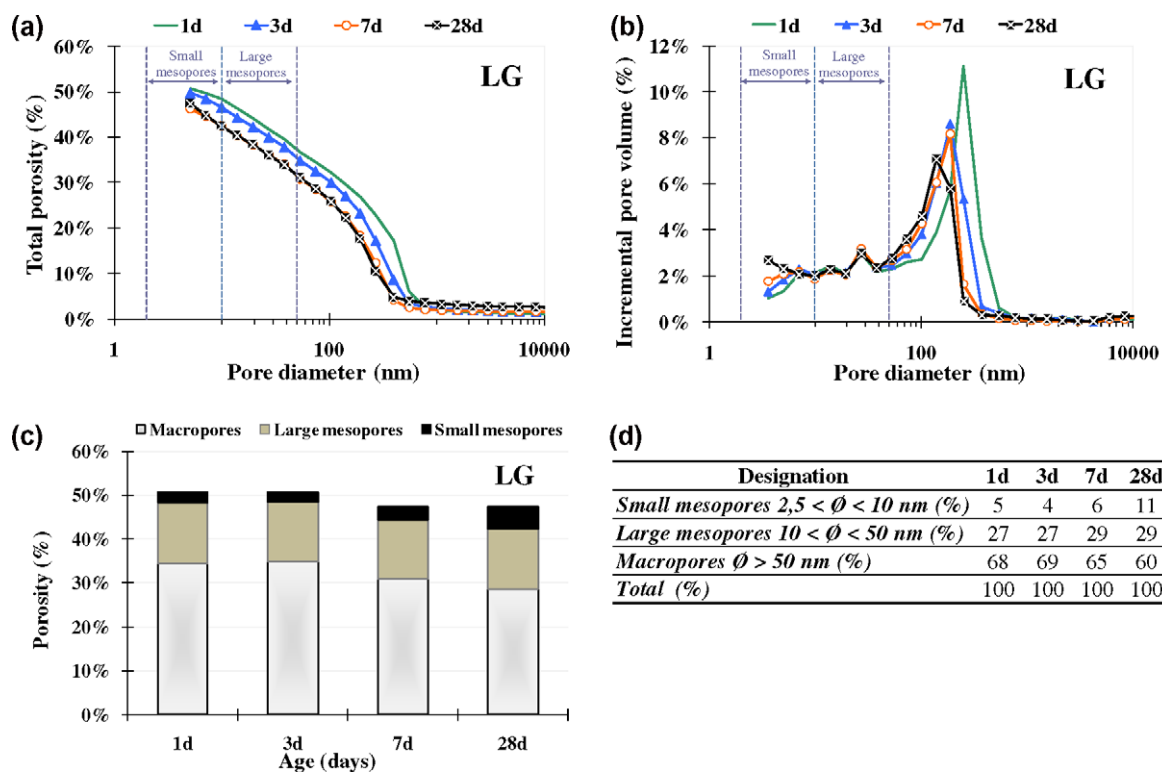


Fig. 6. Porosity (a), incremental pore size (b), porosity distribution (c) and percentile frequency of LG mixture in 1, 3, 7 and 28 days.

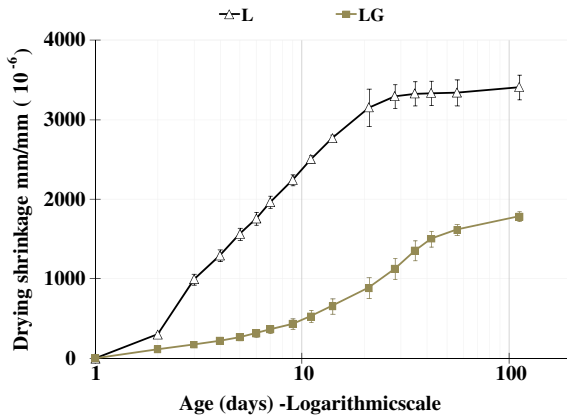


Fig. 8. Drying shrinkage of L and LG mortars.

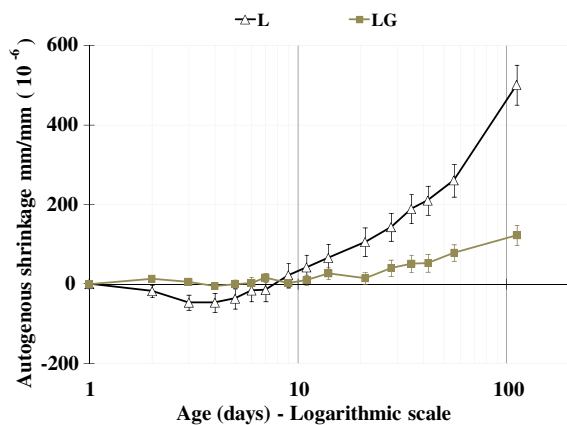


Fig. 9. Autogenous shrinkage of L and LG mortars.

The L mixture produced nearly twice as much drying shrinkage as the LG mixture, which can be explained by porosity and nature of the hydrated products. Fig. 10 presents the evolution of mass changes during the drying shrinkage testing. Most of the water present in the LG and L mortars was not chemically combined to the hydration products in the early ages, being lost due to evaporation (Fig. 10) and, consequently, caused drying shrinkage. The amount of water evaporation in the LG mixture was similar to that observed for the L mixture, however, the LG mixture presents a greater volume of macropores, generating less capillary pressure.

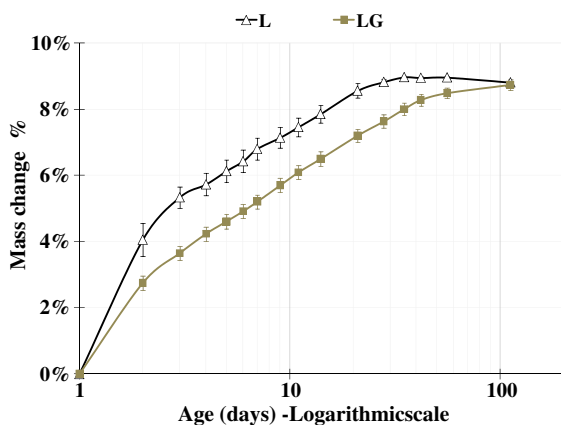


Fig. 10. Mass change of L and LG mixtures.

4. Conclusions

The main conclusions of this study are:

- The cumulative heat from hydration for the slag activated by lime and gypsum (LG) was greater than for slag activated by lime only (L), due to the formation of ettringite and its subsequent transformation in monosulfoaluminate. However, the results obtained in both mixtures are lower than those reported by ordinary Portland cement.
- Thermogravimetric analysis revealed a higher mass loss for slag activated by lime and gypsum (LG) between 30 °C and 220 °C, mostly attributed to the dehydration of ettringite. The slag activated by lime only (L) shows a mass loss peak for C–S–H, aluminate phases, portlandite and calcium carbonate. The amount of ettringite formed in the mixture activated by lime and gypsum (LG) is the main difference between the mixes.
- The porosities of the L and LG mixtures were similar, yet the L mixture shows a greater pore refinement with an increase in mesopores volume with age. The mesopores volume of the L mixture was around 57% larger than that in the LG mixture, having a direct effect on mechanical properties and shrinkage. The pore size distribution in LG mixture is more open than in L mixture, confirmed by the macropore volume of the LG mixture, which was around 60% in 28 days, compared to around 37% observed in the mixture L.
- The compressive strength of the L mixture was greater than that of the LG mixture. This behavior is a consequence of the reduced macropore volume resulting from activation of the slag by lime when compared with the activation of the slag by lime plus gypsum. The compressive strength of the L mixture was around 34% higher than in the LG mixture, reaching 35 MPa in 28 days.
- The drying shrinkage of the L mixture was greater than in the LG mixture. This can be attributed to the more refined porous structure in comparison to the LG mixture and the nature of the hydrated products, characterized by the predominance of CSH. Besides the pore size distribution, the nature of the hydrated products also contributes to explain the greater autogenous shrinkage of the L mixture, because it has also a greater effect of self-desiccation on the chemical shrinkage.

References

- [1] Regourd M. Structure and behavior of slag Portland cement hydrates. In: 7th International congress on the chemistry of cement, vol. 1. Paris; 1980. p. 10–26.
- [2] Talling B, Brandstetr J. Present state and future of alkali-activated slag concretes. In: Concrete, proceedings of the third international conference, vol. 2. Trondheim, Norway, ACI SP114; 1989. p. 1519–45.
- [3] Glukhovskiy VD. Ancient, modern and future concretes. In: 1st International conference: alkaline cements and concretes, Kiev, Russia; 1994. p. 1–9.
- [4] Krivenko PV. Alkaline cements. In: 1st International conference: alkaline cements and concretes, Kiev, Russia; 1994. p. 11–129.
- [5] Wang SD, Scrivener KL. Hydration products of alkali activated slag cement. *Cem Concr Res* 1995;25(3):561–71.
- [6] Kumar S, Kumar R, Bandopadhyay A, Alex TC, Kumar BR, Das SK, et al. Mechanical activation of granulated blast furnace slag and its effect on the properties and structure of Portland slag cement. *Cem Concr Compos* 2008;30(8):679–85.
- [7] Roy DM. Alkali-activated cements: opportunities and challenges. *Cem Concr Res* 1999;29(2):249–54.
- [8] Melo Neto AA, Cincotto MA, Repette WL. Drying and autogenous shrinkage of pastes and mortars with activated slag cement. *Cem Concr Res* 2008;38(4):565–74.
- [9] Melo Neto AA. Shrinkage of alkali-activated slag. Master Science Thesis – Escola Politécnica, Universidade de São Paulo, São Paulo; 2002. 180p [in Portuguese].
- [10] Melo Neto AA. Effect of shrinkage compensating and reducing admixtures in alkali activated slag mortars and pastes. PhD Thesis – Escola Politécnica, Universidade de São Paulo, São Paulo; 2007. 253p [in Portuguese].
- [11] Gram HE. Durability of natural fibres in concrete. Stockholm: Swedish Cement and Concrete Research Institute; 1983.

- [12] Bentur A, Akers SAS. The microstructure and ageing of cellulose fibre reinforced cement composites cured in a normal environment. *Int J Cem Compos Lightweight Concr* 1989;11(2):99–109.
- [13] Tolêdo Filho RD, Scrivener KL, England GL, Ghavami K. Durability of alkali-sensitive sisal and coconut fibres in cement mortar composites. *Cem Concr Compos* 2000;22(2):127–43.
- [14] Savastano H, Warden PG, Coutts RSP. Ground iron blast furnace slag as a matrix for cellulose–cement materials. *Cem Concr Compos* 2001;23(4–5):389–97.
- [15] Agopyan V, Savastano H, John VM, Cincotto MA. Developments on vegetable fibre–cement based materials in São Paulo, Brazil: an overview. *Cem Concr Compos* 2005;27(5):527–36.
- [16] Oliveira CTA, John VM, Agopyan, V. Pore water composition of activated granulated blast furnace slag cements pastes. In: *Proceedings 2nd international conference on alkaline cements and concretes*, Kiev State Technical University of Construction and Architecture; 1999. 9p.
- [17] Oliveira CTA. Pore water composition of blast-furnace slag cements. PhD Thesis – Escola Politécnica, Universidade de São Paulo, São Paulo; 2000. 162p [in Portuguese].
- [18] John VM, Cincotto MA, Sjöstrom C, Agopyan V, Oliveira CTA. Durability of slag mortar reinforced with coconut fibre. *Cem Concr Compos* 2005;27(5):565–74.
- [19] Taylor HFW. *Cement chemistry*. 2nd ed. Thomas Telford House; 1997. p. 480.
- [20] Snelson DG, Wild S, O'Farrell M. Heat of hydration of Portland cement–metakaolin–fly ash (PC–MK–PFA) blends. *Cem Concr Res* 2008;38(6):565–74.
- [21] John VM. Cements from slag activated with sodium silicate. PhD Thesis – Escola Politécnica, Universidade de São Paulo, São Paulo; 1995. 189p [in Portuguese].
- [22] Paglia CSB, Wombacher FJ, Böhni HK. Influence of alkali-free and alkaline shotcrete accelerators within cement systems: hydration, microstructure, and strength development. *ACI Mater J* 2004;101(5):353–7.